A 24-28 GHz Tunable LNA in 22nm FDSOI Technology

Sandra George
Barkhausen Institut
Dresden, Germany
sandra.george@barkhauseninstitut.org

Mengqi Cui
Technische Universität Dresden
Dresden, Germany
mengqi.cui@tu-dresden.de

Padmanava Sen
Barkhausen Institut
Dresden, Germany
padmanava.sen@barkhauseninstitut.org

***Abstract*—This paper presents a $26\,\mathrm{GHz}$ tunable low noise amplifier (LNA) in 22nm FDSOI technology implemented for 5G NR at $24\,\mathrm{GHz}$-$28\,\mathrm{GHz}$ band. The LNA employs a 2-stage cascaded common source topology with inductive degeneration for input matching. For a power consumption of $13.2\,\mathrm{mW}$ from $800\,\mathrm{mV}$ voltage supply, the LNA provides a peak measured gain of $14.7\,\mathrm{dB}$ and a noise figure of $3.15\,\mathrm{dB}$. The LNA achieves a maximum input 1-dB compression point of $-12\,\mathrm{dBm}$ at $24\,\mathrm{GHz}$ with an overall area of $0.26\,\mathrm{mm}^2$. The multi-band operation is attained through interstage and output tuning using varactors. This tunability facilitates the LNA to block out-of-band interferers that can affect the linearity and sensitivity of the radio frequency (RF) front-ends. Additionally, the tunability in matching makes the integration of LNA in RF front-ends easier. The demonstrated LNA is an essential building block of a reconfigurable front-end that will be key enabler for hardware reuse in future 6G applications.**

***Index Terms*—LNA, FDSOI, millimeter-wave integrated circuits**

I. Introduction

Fifth generation (5G) communication standards and systems have been developing rapidly in the recent years motivated by the high demand for increased data rate. The $24.25\,\mathrm{GHz}$-$27.5\,\mathrm{GHz}$ spectrum is currently proposed for the 5G standard communication links. The 5G communication technologies has been significantly enhancing the performance of wireless communication systems which makes mmWave high performance low noise amplifiers (LNA)s also on high demand [1]. While, the mmWave and sub THz systems have been projected to be of utmost importance in future 6G systems, reconfigurability/tunability of hardware will play an important role to meet the diversity of needs enabling reuse of hardware, when possible [2]. With reprogrammable circuitry, not only the communication networks, joint radio communications and sensing (JC&S) can also be supported in future networks, driven by new use cases [3].

The LNA operation is a determining factor in the system sensitivity. With further developments in wireless communication technologies, multi-standard RF receiver front-ends that work in a multi-band, multi-mode configuration will become a key enabler for future 6G systems. In any wideband system, one must be concerned about the large interferers that can pass through the broad-band matching networks. These out-of-band blockers in a wideband LNA can cause decreased RF front-end sensitivity owing to the additional noise and they can also increase the linearity requirements of the RF blocks. A multi-band LNA operating in multiple narrow bands ensures reduction in noise and interfering signals leading to high selectivity and increased sensitivity of the receiver.

Frequency tunablity can be achieved by tuning the input and output matching networks of the LNA [4]. This paper looks at specific designs that can bring tunability in an inductively degenerated common source topology. Some common techniques for tunability include the use of switched multi-tap transformer based inductors [5] [6], switched LC tanks [5] and varactors [7]. The switching elements in the switched circuits bring in non-linearities associated with its parasitic capacitance and can cause a change in the resonant frequency. Continuous tunability is preferred over discrete tuning as it is less sensitive to process variations and this architecture enables tunability which can mitigate matching variabilities to an extent [8]. A varactor based tuning was adopted in this paper to enable continuous tuning and eliminate any non-linearities associated with the switch. It also enables a compact design with no additional power consumption, without impacting the overall LNA performance.

The $22\,\mathrm{nm}$ Fully Depleted Silicon On Insulator (FDSOI) technology offers high performance mm-Wave devices in terms of $\mathrm{f_T}$, $\mathrm{f_{max}}$ and $\mathrm{NF_{min}}$ and offers high integration which would result in low system costs. This makes the technology a perfect candidate for RF front-end integration.

In this work, a tunable LNA is proposed for 24-28 GHz which provides a minimum noise figure (NF) of 3.15 dB. The LNA has a 3dB RF bandwidth of $7.5\,\mathrm{GHz}$ (21.3-28.8 GHz) covering the entire 5G NR band. Section II covers the design and implementation of the circuit. Section III presents the simulation and measurement results followed by the comparison to state-of-the-art SOI LNAs in Section IV and then, the conclusion is provided.

II. Circuit Design and Implementation

The LNA is designed in $22\,\mathrm{nm}$ FDSOI technology from GlobalFoundries which provides 10 layers of Copper and one Aluminium top metal layers. This designs employs super-low Vt (slvt) NMOS transistors because of its low noise and high $\mathrm{f_T}/\mathrm{f_{max}}$ characteristics.

This work is financed on the basis of the budget passed by the Saxon State Parliament.

DOI 10.1109/ICECS58634.2023.10382880

The schematic view of the LNA is presented in Fig. 1. The transistors (M_1 and M_2) are biased closed to NF_{min} at a current density of $0.2\,mA/\mu m$. The NF_{min} was attained around $0.45\,V$ gate bias voltage and hence it was chosen as the nominal bias voltage for the transistors.

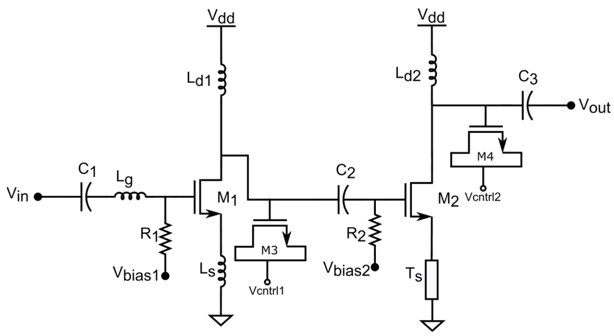

Fig. 1: Schematic view of 26GHz tunable LNA

The series gate resistance (R_g) of the transistor is one of the major contributors to the overall noise of the LNA. In this design, in order to reduce the gate resistance, 8 transistors of $5\,\mu m$ width are connected in parallel instead of a single device with large number of fingers. Each transistor uses 10 fingers with $500\,nm$ finger width. M1 to C3 metal layers were stacked and the thick and low loss C3 metal layer was used for routing to further decrease R_g. Total width of the transistors used in this design in $40\,\mu m$.

Foundry inductors (L_g, L_s, L_{d1}, L_{d2}) and alternate-polarity-metal-oxide-metal (APMOM) capacitors (C_1, C_2, C_3) from the mm-Wave libraries were used for matching purposes. All inductors except L_g has a quality factor (Q) of at least 20 and the inductor L_g provides a Q factor of 14. The inductors used are all single-ended in nature. The degeneration inductor at the second stage, T_s was realised by a transmission line with bottom ground shield. The varactors, M_3 and M_4 were also from the mm-Wave library. The actual values of all the components used in this design is detailed in Table I.

TABLE I: Component values

L_g	L_s	L_{d1}	L_{d2}	C_1
781 pH	191 pH	178 pH	206 pH	569.5 fF
C_2	C_3	M_1, M_2	M_3, M_4	
1.3 pF	108 fF	$40\,\mu m/20\,nm$	$1\,\mu m/100\,nm$	

The ground and VDD planes were designed as grids with upper metal layers and the supply decoupling capacitors were designed using APMOM capacitors and placed as grids.

The LNA uses inductive degeneration for input matching the transistor to $50\,\Omega$. A cascode configuration was avoided to minimize the overall noise contribution. The output of the first stage is resonated with the total capacitance seen at the input of M_2. This simplifies the interstage matching of the LNA. The output was also matched to $50\,\Omega$ using an L matching network. The previous tapeouts showed process variations and parasitic effects which resulted in a frequency shift of S11 and S22 matching. By adding varactors, we were able to alleviate these process variations while achieving multi-band operation. Two MOS NCAP varactors (M_3, M_4) were used to facilitate input and output tuning.

III. Simulation and Measurement Results

The LNA was fabricated in GlobalFoundries 22nm FDSOI process and occupies a total space of $0.26\,mm^2$ and $0.13\,mm^2$ with and without pads respectively. The chip as shown in Fig. 2 was measured using vector network analyzer Rohde & Schwarz ZVA-67.

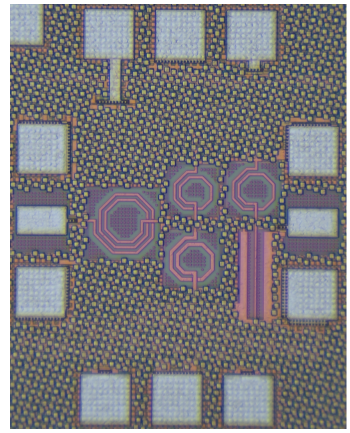

Fig. 2: Micrograph of 26GHz LNA

The S parameter measurements for varactor voltages V_{cntrl1}=0.4 V and V_{cntrl2}=0.5 V are shown in Fig. 3. The input and output return losses (S11 and S22) are below $-10\,dB$ from 24 GHz-28 GHz. The maximum gain attained for this configuration is $13\,dB$ at $24\,GHz$. The $3\,dB$ BW is $7.5\,GHz$ and the current consumed from $0.8\,V$ supply is $16.5\,mA$.

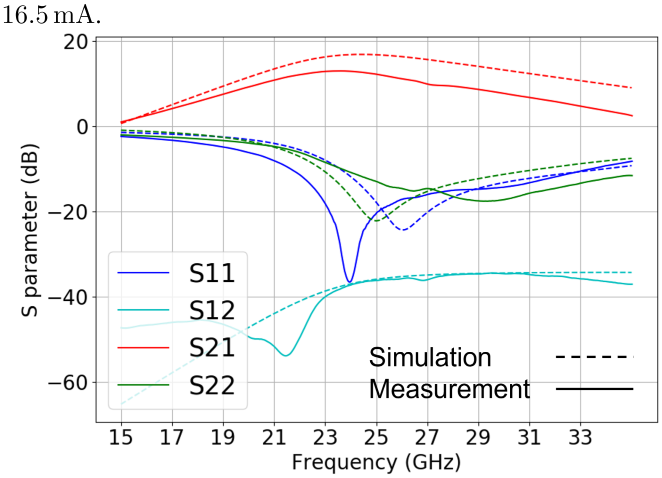

Fig. 3: Measured and simulated S-parameters of the LNA at varactor V_{cntrl1}=0.4 V and V_{cntrl2}=0.5 V

Fig. 4 shows the variability in tuning of the LNA with change in varactor control voltages. The varactor control voltage combinations, 1-9 selected for the measurements are listed in Table II. The peak measured gain attained by the LNA is $14.7\,dB$ at V_{cntrl1}=0.8 V and V_{cntrl2}=0.8 V with unconditional stability. The measured varactor tunability is not as pronounced as in the simulations and we attribute it to the parasitic inductance associated with the control voltage lines. This adds to future improvements in the design in terms of tunability. The diminishing trend of S21 across the tuning range at lower frequencies can be compensated at the subsequent mixer stage which usually has higher coversion gains at lower frequencies in the band.

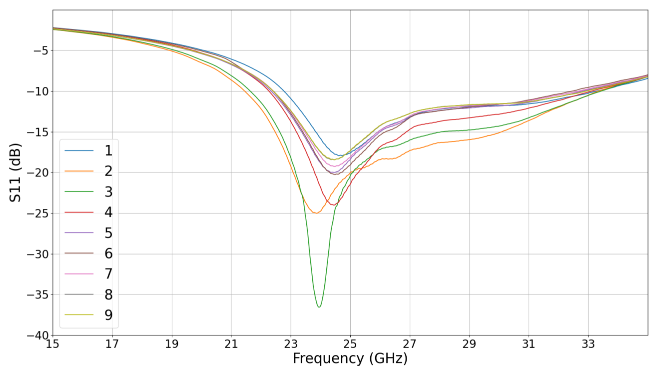

(a)

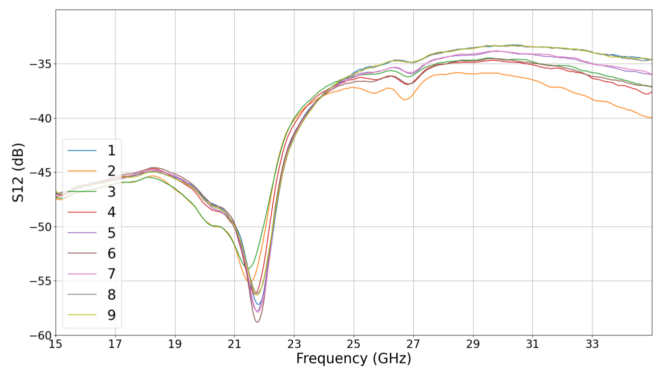

(b)

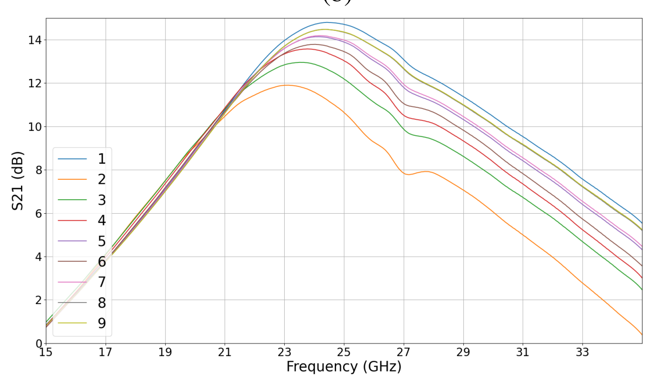

(c)

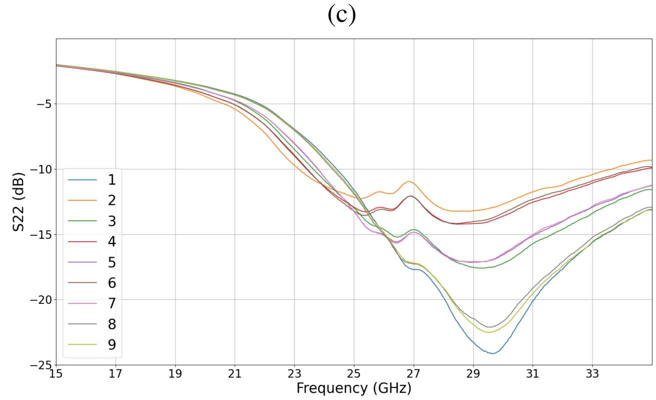

(d)

Fig. 4: Measured (a) S11, (b) S12, (c) S21 and (d) S22 of the LNA at different varactor control voltage combinations (refer Table II)

To ensure that the LNA meets the specifications at different and extreme process variations, corner simulations were performed at different varactor voltages. The operational bandwidth where S11 and S22 are below $-10\,\mathrm{dB}$ and the gain is within the 3-dB bandwidth, were studied. The simulations showed that the LNA is able to meet the tunability requirements across the frequency band with changes in varactor control voltages at different corners.

The NF of the LNA was measured using Y-method with signal and spectrum analyzer Rohde & Schwarz FSW-67 and a calibrated noise source Noisecom NC346V. Fig. 5 shows the measured and simulated NF of the LNA across the frequency band. The minimum measured NF attained is $3.15\,\mathrm{dB}$ at $24\,\mathrm{GHz}$ whereas the NF at $26\,\mathrm{GHz}$ is $3.37\,\mathrm{dB}$. The LNA achieves a IP1dB compression at $-13.8\,\mathrm{dBm}$ at $26\,\mathrm{GHz}$ as shown in Fig. 6. The measured IP1dB compression point of the LNA across the band is shown in Fig. 7 and the highest compression point of $-12\,\mathrm{dBm}$ was attained at $25\,\mathrm{GHz}$ in the 5G NR frequency band.

TABLE II: Varactor voltages used in measurements

	V_{cntrl1} (V)	V_{cntrl2} (V)		V_{cntrl1} (V)	V_{cntrl2} (V)
1	0.8	0.8	2	0.2	0.2
3	0.4	0.5	4	0.5	0.4
5	0.6	0.5	6	0.7	0.4
7	0.8	0.5	8	0.8	0.6
9	0.8	0.7			

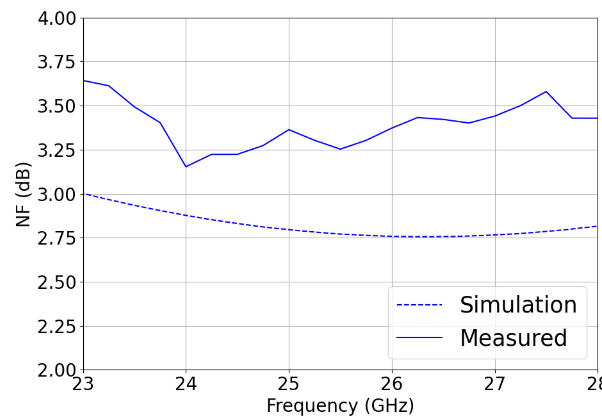

Fig. 5: Simulated and measured NF of the LNA across the frequency band

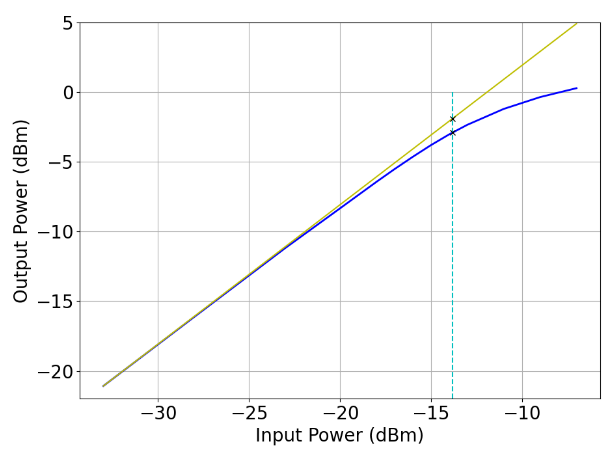

Fig. 6: Measured linearity characteristics of the LNA at 26GHz

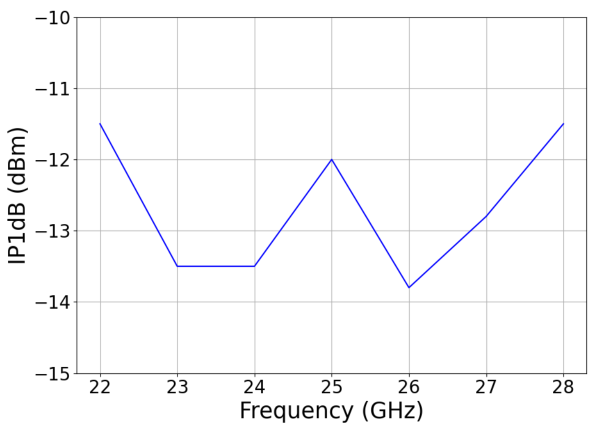

Fig. 7: Measured P1dB points across the frequency band

IV. Comparison to state of the art SOI LNAs in the 5G NR band

The comparison of the LNA with other state-of-the-art LNAs in similar frequency bands and technology are shown in Table III. The LNA compares well with other state-of-the-art LNAs. Compared to [1] which has a similar power consumption, this LNA achieves a similar gain and P1dB compression point. The improvement can be in case of the NF, which we attribute to the multi-stage design. Other designs make use of multi-stage cascode structures, which contribute to the higher gains. The LNA has a high IP1dB compression point while consuming low power. Many of the LNAs listed in the table are wideband LNAs and hence FOMs without bandwidth as a parameter are selected while making sure all LNAs meet the percentage bandwidth requirement for the intended application. The FOM was determined using (1) . The FOM of the LNA is

$$\mathrm{FoM} = \frac{\mathrm{Gain[lin].P1dB[mW]}}{\mathrm{Pdc[mW].(NF[lin]-1)}} \tag{1}$$

The achieved FOM is comparable to the previously reported works.

V. Conclusion

This article presented a 24 GHz-28 GHz 2-stage common source LNA for the mm-wave 5G NR band in 22nm FDSOI technology. The frequency tunable LNA provides a low NF of 3.15 dB and a peak measured gain of 14.7 dB with a 3dB bandwidth of 7.5 GHz while consuming a power of 13.2 mW. This makes the propoed LNA a good candidate for the integration in front-end modules while mitigating the process variations in matching with a mixer. The primary contribution of this article is to demonstrate with measurements, a design methodology for tunability/reconfigurability of LNA, a critical block in any receiver front-end. The design methodologies proposed in this work are extendable towards higher frequency bands (e.g. 60 GHz ISM bands) to meet future 6G front-end requirements.

TABLE III: Comparison of this work to 5G NR band LNAs in SOI process

	This work	[1]	[9]	[10]	[11]	[12]
Tech	22nm FDSOI	22nm FDSOI	45nm SOI	22nm FDSOI	22nm FDSOI	45nm SOI
Supply (V)	0.8	1.3	1.1	1.05	1, 1.6	1
Frequency (GHz)	24-28	19-34	28	22-32	24-43	20-40
3dBBW (GHz)	7.5	16.7	-	17	19	20
Gain (dB)	14.7	12.6	24	21.5	23	21.2
NF(dB)	3.15	1.35	4	1.9	3-7	2.5-3
IP1dB (dBm)	-12	-7.9	-23	-23.4*	-21	-20 - -17
P_{dc} (mW)	13.2	13	18.5	17.3	20.5	18
Area (mm^2)	0.26	0.21	0.15 w/o pads	0.17	0.46	0.675
FOM	0.132	0.622	0.045	0.068	0.077	0.187

*Estimated from IIP3

References

[1] C. Zhang, F. Zhang, S. Syed, M. Otto and A. Bellaouar, "A Low Noise Figure 28GHz LNA in 22nm FDSOI Technology," 2019 IEEE Radio Frequency Integrated Circuits Symposium (RFIC), 2019, pp. 207-210, doi: 10.1109/RFIC.2019.8701831.

[2] I. F. Akyildiz, A. Kak and S. Nie, "6G and Beyond: The Future of Wireless Communications Systems," in IEEE Access, vol. 8, pp. 133995-134030, 2020, doi: 10.1109/ACCESS.2020.3010896.

[3] G. P. Fettweis and H. Boche, "6G: The Personal Tactile Internet—And Open Questions for Information Theory," in IEEE BITS the Information Theory Magazine, vol. 1, no. 1, pp. 71-82, 1 Sept. 2021, doi: 10.1109/MBITS.2021.3118662.

[4] A. Aneja and X. J. Li, "Multiband LNAs for Software-Defined Radios: Recent Advances in the Design of Multiband Reconfigurable LNAs for SDRs in CMOS, Microwave Integrated Circuits Technology," in IEEE Microwave Magazine, vol. 21, no. 7, pp. 37-53, July 2020, doi: 10.1109/MMM.2020.2985189.

[5] C. Fu, C. Ko, C. Kuo and Y. Juang, "A 2.4–5.4-GHz Wide Tuning-Range CMOS Reconfigurable Low-Noise Amplifier," in IEEE Transactions on Microwave Theory and Techniques, vol. 56, no. 12, pp. 2754-2763, Dec. 2008, doi: 10.1109/TMTT.2008.2006804.

[6] X. Yu and N. M. Neihart, "A 2–11 GHz reconfigurable multi-mode LNA in 0.13µm CMOS," 2012 IEEE Radio Frequency Integrated Circuits Symposium, 2012, pp. 475-478, doi: 10.1109/RFIC.2012.6242325.

[7] Z. Wang et al., "A Ka-Band Switchable LNA With 2.4-dB NF Employing a Varactor-Based Tunable Network," in IEEE Microwave and Wireless Components Letters, vol. 31, no. 4, pp. 385-388, April 2021, doi: 10.1109/LMWC.2021.3059655.

[8] M. El-Nozahi, E. Sanchez-Sinencio and K. Entesari, "A CMOS Low-Noise Amplifier With Reconfigurable Input Matching Network," in IEEE Transactions on Microwave Theory and Techniques, vol. 57, no. 5, pp. 1054-1062, May 2009, doi: 10.1109/TMTT.2009.2017249.

[9] V. Chauhan and B. Floyd, "A 24–44 GHz UWB LNA for 5G Cellular Frequency Bands," 2018 11th Global Symposium on Millimeter Waves (GSMM), 2018, pp. 1-3, doi: 10.1109/GSMM.2018.8439672.

[10] B. Cui and J. R. Long, "A 1.7-dB Minimum NF, 22–32-GHz Low-Noise Feedback Amplifier With Multistage Noise Matching in 22-nm FD-SOI CMOS," in IEEE Journal of Solid-State Circuits, vol. 55, no. 5, pp. 1239-1248, May 2020, doi: 10.1109/JSSC.2020.2967548.

[11] L. Gao and G. M. Rebeiz, "A 24-43 GHz LNA with 3.1-3.7 dB Noise Figure and Embedded 3-Pole Elliptic High-Pass Response for 5G Applications in 22 nm FDSOI," 2019 IEEE Radio Frequency Integrated Circuits Symposium (RFIC), 2019, pp. 239-242, doi: 10.1109/RFIC.2019.8701782

[12] M. Lokhandwala, L. Gao and G. M. Rebeiz, "A High-Power 24–40-GHz Transmit–Receive Front End for Phased Arrays in 45-nm CMOS SOI," in IEEE Transactions on Microwave Theory and Techniques, vol. 68, no. 11, pp. 4775-4786, Nov. 2020, doi: 10.1109/TMTT.2020.2998011.